Proc. Natl. Acad. Sci. USA
Vol. 92, pp. 10232–10236, October 1995
Biochemistry

Crystal structure of the cell cycle-regulatory protein suc1 reveals a β-hinge conformational switch

YVES BOURNE*†, ANDREW S. ARVAI*, SUSAN L. BERNSTEIN*, MARK H. WATSON*, STEVEN I. REED*, JANE E. ENDICOTT‡, MARTIN E. NOBLE‡, LOUISE N. JOHNSON‡, AND JOHN A. TAINER*

*The Scripps Research Institute, MB4, 10666 North Torrey Pines Road, La Jolla, CA 92037; and ‡Laboratory of Molecular Biophysics, University of Oxford, South Parks Road, Oxford OX1 3QU, United Kingdom

Communicated by David Eisenberg, University of California, Los Angeles, CA, July 21, 1995 (received for review February 25, 1995)

ABSTRACT **The *Schizosaccharomyces pombe* cell cycle-regulatory protein suc1, named as the suppressor of cdc2 temperature-sensitive mutations, is essential for cell cycle progression. To understand suc1 structure–function relationships and to help resolve conflicting interpretations of suc1 function based on genetic studies of suc1 and its functional homologs in both lower and higher eukaryotes, we have determined the crystal structure of the β-interchanged suc1 dimer. Each domain consists of three α-helices and a four-stranded β-sheet, completed by the interchange of terminal β-strands between the two subunits. This β-interchanged suc1 dimer, when compared with the β-hairpin single-domain folds of suc1, reveals a β-hinge motif formed by the conserved amino acid sequence HVPEPH. This β-hinge mediates the subunit conformation and assembly of suc1: closing produces the intrasubunit β-hairpin and single-domain fold, whereas opening leads to the intersubunit β-strand interchange and interlocked dimer assembly reported here. This conformational switch markedly changes the surface accessibility of sequence-conserved residues available for recognition of cyclin-dependent kinase, suggesting a structural mechanism for β-hinge-mediated regulation of suc1 biological function. Thus, suc1 belongs to the family of domain-swapping proteins, consisting of intertwined and dimeric protein structures in which the dual assembly modes regulate their function.**

Cell cycle regulation requires highly regulated cooperative transitions to be provided by the interactions of several proteins with the catalytically active cyclin-dependent kinase (Cdk) (for recent reviews, see refs. 1–3), including suc1 (4–8). Yet, significant questions exist regarding both suc1 structure and biological function. Whereas conserved sequence regions have been identified among suc1 proteins from yeast to man (9–11) (Fig. 1*A*), no functionally important structural motif for Cdk binding has been elucidated. Although suc1 is essential for cell cycle progression *in vivo* and clearly interacts genetically and physically with Cdks (4, 12–14), its precise biological function has remained elusive. Conflicting results on suc1 activity have been obtained from biochemical studies and genetic experiments involving gene disruption (12–15), overexpression (16, 17), and temperature-sensitive mutants of a suc1 homolog (4, 11), as well as suppression of temperature-sensitive cdc2 mutants (4, 12, 13, 15). Both positive (12–15) and negative (17) effects on cell cycle progression have been attributed to suc1, and some of these apparent conflicts might be reconciled if the same suc1 protein adopts more than one functionally distinct form.

Here we establish the existence of two distinct thermodynamically stable forms of suc1. Further, we present the atomic structure of the β-interchanged dimeric suc1§ and use comparative analysis with the recently determined crystal structures of the β-hairpin single domain monomeric suc1 (18) and its human homolog CksHs2 (19) to identify a β-hinge motif defined by residues His^{88}–His^{93}. The conformation of the β-hinge motif controls suc1 fold, assembly, and conserved molecular surface accessible for cdc2 kinase recognition. Our two suc1 structures reveal that opening the β-hinge motif causes β-strand domain swapping to occur in this essential cell cycle protein. So far this dual mode of quaternary structure has been observed in only a few oligomeric proteins, such as the seminal RNase (20) and diphtheria toxin (21).

METHODS

Escherichia coli BL-21 cells containing suc1 expression plasmid pRK171 were grown at 37°C in LB medium with ampicillin (100 μg/ml) until an OD_{600} of 0.5–0.6 was reached. The bacteria were then induced with 0.4 mM isopropyl β-D-thiogalactopyranoside and grown for an additional 2–3 hr. Cells were then harvested by centrifugation at 6000 × *g* for 15 min. The supernatant was discarded and cell pellets were frozen in liquid nitrogen and stored at −70°C. Cell pellets were lysed in 20 mM Hepes, pH 7.0/2 mM EDTA/1 mM 2-mercaptoethanol/1 mM phenylmethanesulfonyl fluoride (DEAE buffer) with sonication. Cell debris and DNA were removed by centrifugation. The supernatant was directly applied to a Pharmacia DEAE-Sepharose Fast Flow column equilibrated with DEAE buffer and was eluted with a 0–0.5 M NaCl gradient. suc1-containing fractions were dialyzed against 25 mM imidazole·HCl (pH 7.0) and applied to a Pharmacia PBE 94 chromatofocusing column. Fractions were eluted with Polybuffer 74, 1:8 dilution at pH 4.0. suc1-containing fractions were eluted around pH 5.4. These fractions were pooled, concentrated, and then applied to a Pharmacia Sepharose 200 column equilibrated in 50 mM Tris·HCl, pH 8.0/150 mM NaCl/1 mM EDTA/1 mM 2-mercaptoethanol. Two peaks were eluted from this column, apparently corresponding to a suc1 monomer and dimer, respectively. For crystallization experiments, the dimer peak fractions were pooled, dialyzed into 5 mM imidazole/malate (pH 7.4), and concentrated to 10 mg/ml over a membrane with a molecular weight cutoff of 3000.

Crystals of suc1 dimer were obtained by vapor diffusion techniques at 20°C with 20% PEG-4000, 5% (from a saturated solution) LiCl, and 100 mM imidazole/malate (pH 6.6). The crystals belong to the space group $P2_12_12_1$ with cell dimensions: $a = 55.7$ Å, $b = 85.6$ Å, $c = 97.7$ Å, giving the V_m value (22) of 2.2 Å^3/Da (50% solvent) for four suc1 molecules in the

The publication costs of this article were defrayed in part by page charge payment. This article must therefore be hereby marked "*advertisement*" in accordance with 18 U.S.C. §1734 solely to indicate this fact.

Abbreviations: rmsd, root-mean-square deviation; Cdk, cyclin-dependent kinase.

†Permanent address: Centre National de la Recherche Scientifique, Institut Fédératif de Recherche Concertée 1, Laboratoire de Cristallisation et de Cristallisation des Macromolécules Biologiques, 31 Ch. J. Aiguier, 13402 Marseille Cedex 20, France.

§The atomic coordinates have been deposited in the Protein Data Bank, Chemistry Department, Brookhaven National Laboratory, Upton, NY 11973 (reference 1SCE).

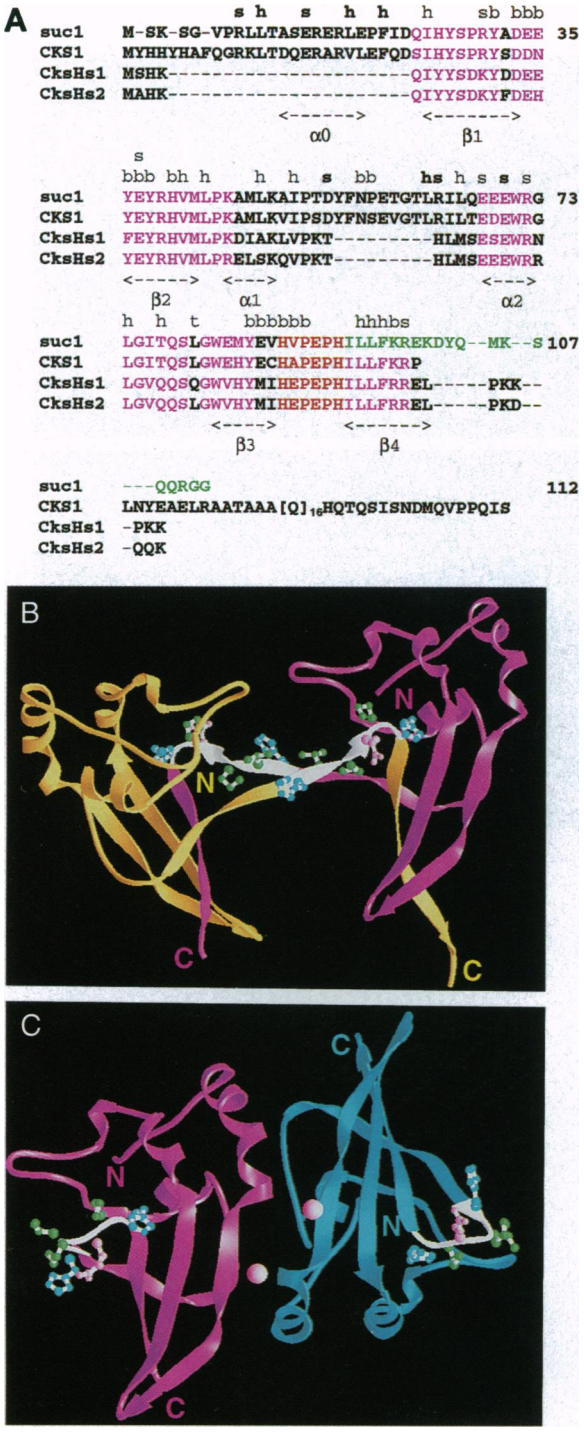

FIG. 1. suc1 fold, secondary structure, sequence conservation, and conformational switch. (*A*) The sequences of the two yeast homologs (suc1 and CKS1) are aligned with those of the two human proteins (CksHs1 and CksHs2). The β-hinge region His^{88}–His^{93} (red), which forms a β-bend between β3 and β4 in the β-hairpin single-domain fold (18), is sequence-conserved but is conformationally different in the β-interchanged suc1 dimer reported here. Residues conserved in suc1 proteins are highlighted (magenta). The β-strand involved in domain swapping for the β-interchanged suc1 dimer structure presented here is also represented (green). The zinc ion is bound to residues Asp^{23}, His^{26}, and His^{40} in the crystal structure of the suc1 β-hairpin single-domain fold (18). Residue functions implied by the new β-interchanged dimer structure are identified by symbols: b, buried residue in the β-interchanged suc1 dimer; h, hydrophobic cluster conserved among suc1 homologs; **h**, additional suc1 hydrophobic cluster; s, salt bridge conserved among suc1 homologs; **s**, additional suc1 salt bridge; d, buried hydrophobic residue in the β-interchanged suc1 dimer; t, buried hydrophobic residue at the tetramer interface. (*B*) β-Interchanged suc1 dimer fold (yellow and magenta subunits) reported here. The side chains forming the β-hinge region (His^{88} to His^{93}; white backbone) are displayed as balls and sticks (white bonds): His^{88} and His^{93} (blue spheres); Val^{89}, Pro^{90}, and Pro^{92} (green spheres); Glu^{91} (pink spheres). (*C*) suc1 β-hairpin single domain fold (18) (magenta and blue subunits) with zinc-promoted (pink spheres) weak dimer. The β-hinge region is displayed as in *B*. Figs. 1*B*, 1*C*, and 2*A* were generated using RIBBONS (27).

asymmetric unit. A 2.2-Å-resolution data set that consisted of 49,409 observations for 19,489 unique reflections (83% complete, R_{sym} = 6%) was collected from one crystal by use of the University of California, San Diego, mark II multiwire area detector (23). Initial phases were obtained by molecular replacement using a truncated suc1 molecule (18) as a search model (residues 6–11 and 88–93 removed) with the AMORE program package (24) (version R3.T2.F2.O5). Only one monomer from the zinc-promoted crystallographic suc1 dimer gave the correct orientation. The highest peak in the translation function of one truncated suc1 molecule was automatically used to position the other three molecules with the phased translation function by screening all other rotation peaks. After the fitting procedure on the four molecules, the correlation and the *R* factor were 50% and 43%, respectively, in the 15-Å to 3.5-Å resolution range, with the second solution at 38% and 48%, respectively. Refinement of 6-Å to 2.8-Å data with X-PLOR (25) gave an *R* factor of 35%. The β-hinge region (residues His^{88}–His^{93}) was then built between two symmetry-related suc1 molecules into both $2F_o - F_c$ and $F_o - F_c$ maps with the graphics program TURBO-FRODO (26). Addition of the N and C termini, chloride ions, and water molecules with subsequent refinements without noncrystallographic symmetry restraints gave a final *R* factor of 19.3% for 18,451 reflections (all data) between 6-Å and 2.2-Å resolution, and a free *R* factor of 28.4% (10% of the reflections). The final model comprises residues Val^{6}–Ala^{102}, Val^{6}–Ala^{102}, Ser^{2}–Gly^{112}, and Ala^{3}–Met^{105} for each monomer, respectively. The overall deviations from ideal geometry are 0.008 Å for bond distances and 1.5° for bond angles. For the four suc1 molecules (3655 protein atoms), the root-mean-square deviation (rmsd) is 0.9 Å and 0.7 Å for all atoms including side chains and all C^{α} atoms, respectively, and only 0.65 Å and 0.55 Å for residues Val^{6}–His^{88}. The polypeptide backbone dihedral angles all lie in allowed regions of the Ramachandran diagram. Temperature factors average 26 $Å^2$ for main chains, 28 $Å^2$ for side chains, 18 $Å^2$ for 3 chloride ions, and 35 $Å^2$ for 238 solvent molecules.

RESULTS

In sequence order, the suc1 secondary structure consists of an α-helix, a pair of β-strands, a pair of α-helices, and a pair of C-terminal β-strands. The amino acid sequence and its secondary structure are highly conserved among the suc1 family of proteins, resulting in 53% identity between yeast and human Cks proteins (Fig. 1*A*). Each suc1 domain is folded into a four-stranded antiparallel β-sheet, abutted at the top by three α-helices to form the hydrophobic core. Compared with the human homologs CksHs1 and CksHs2, suc1 additionally contains an N-terminal helix, a small loop in the region joining the two helices, and a C-terminal extension (Fig. 1*A*).

The β-interchanged suc1 dimer domain fold presented here is formed by two interlocked subunits such that the C-terminal β-strand, β4, extends and exchanges with the identical strand from the other subunit in the dimer (Fig. 1*B*). In contrast, the recently determined β-hairpin single-domain suc1 structure crystallized with zinc ions revealed two independently folded monomeric domains joined by a weak zinc-mediated contact (18) (Fig. 1*C*). No clear physiological function has been determined for the zinc, and the zinc ion ligands are not

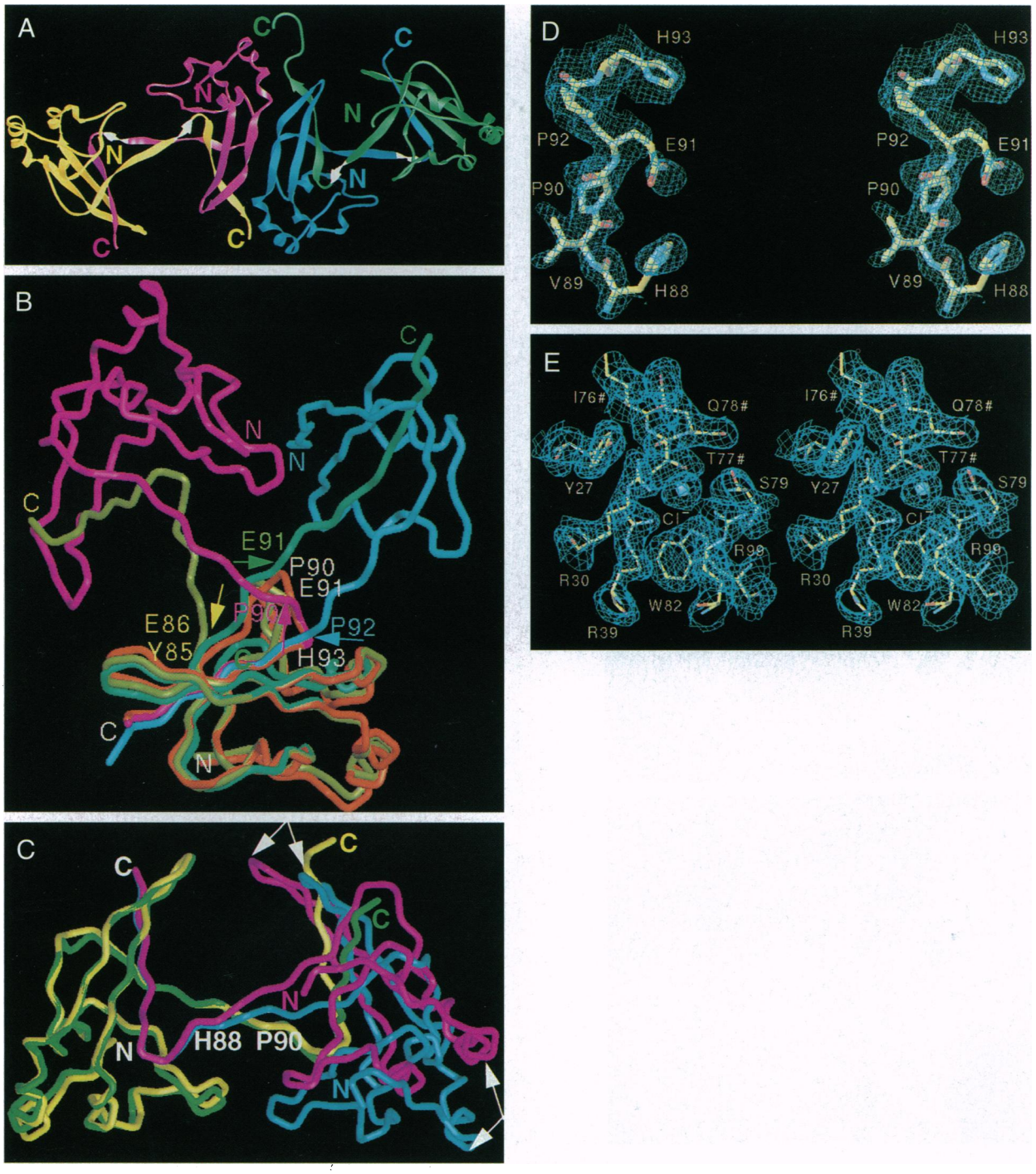

FIG. 2. suc1 fold and assembly. (*A*) Ribbon model of the two β-interchanged suc1 dimers present in the asymmetric unit (yellow and magenta and blue and green subunits). The hinge points are located within residues Pro^{90}–Glu^{91}, which join β3 and β4, are highlighted (white). The N and C termini are labeled. For comparison, the magenta subunit has the same orientation as in Fig. 1 *B* and *C*. The blue subunit is oriented similarly to the zinc-promoted suc1 dimer (18) (Fig. 1*C*) but is translated down by 15 Å in the tetramer interface reported here. (*B*) Superposition of a β-interchanged suc1 dimer (yellow and magenta subunits) with a CksHs2 dimer (19) (blue and green subunits) and the β-hairpin single-domain suc1 (18) (red subunit). Magenta and yellow arrows represent the main hinge points for the β-interchanged suc1 relative to the suc1 β-hairpin single-domain fold (18), as do blue and green arrows for the CksHs2 dimer hinge points. Molecules are superimposed according to the C^{α} atoms of residues Val^{6}–His^{88} and Gln^{5}–His^{60} for yeast and human Cks proteins, respectively. (*C*) Superposition of the two β-interchanged suc1 dimers from the crystallographic asymmetric unit. The locus of the β-hinge region is labeled. The magenta and yellow dimer has the smallest hinge-bending angle. Dimer molecules are superimposed according to the C^{α} atoms of residues Val^{6}–His^{88}. (*D*) Electron density map and model for the well-ordered β-hinge region. Shown is a stereo pair of the 2.2-Å-resolution omit $F_o - F_c$ electron density map contoured at 2.0σ (blue) of the HVPEPH region, where the coordinates of this region were omitted and the protein coordinates were refined by simulated annealing before the phase calculation for the map. (*E*) Electron density map and model for the chloride ion and threonine residue bound to the anion binding site. Shown is a stereo pair of the final $2F_o - F_c$ electron density map contoured at 1.0σ, with colored atoms around the anion binding site. The five invariant residues forming the anion binding site (Arg^{30}, Arg^{39}, Arg^{99}, Ser^{79}, and Trp^{82}) are labeled, together with the chloride ion (light blue sphere). The symbol (#) denotes the residues in the adjacent subunit.

conserved within suc1 proteins (Fig. 1*A*), so this apparently represents a crystal contact interaction between suc1 monomers. The differences in fold and assembly between the β-interchanged dimer (Fig. 1*B*) and the suc1 single-domain monomeric fold (Fig. 1*C*) are primarily in the sequence-conserved β-hinge region His^{88}–His^{93}. Thus, the conserved sequence motif HVPEPH (residues 88–93) forms a β-hinge allowing switching between the suc1 monomer β-hairpin and the β-strand domain swapping seen in the suc1 dimer structure. These two forms are thermodynamically stable at physiological pH and ionic strength and could be purified separately from *E. coli*-expressed protein (see *Methods*). As the variation is localized to the β-hinge, the suc1 core structure and hydrophobic packing are highly conserved between the β-hairpin single-domain monomer (18) and the β-interchanged dimer. The average rmsd is 0.64 Å between the main-chain atoms Val^6–His^{88} and His^{93}–Arg^{99}, where His^{93}–Arg^{99} belongs either to the same monomer or to the adjacent subunit for the closed and opened β-hinge conformation, respectively.

In the crystal structure, pairs of β-interchanged suc1 dimers pack to form a flat elongated tetramer (Fig. 2*A*), consistent with tetrameric associations observed by gel filtration chromatography (data not shown). At the suc1 tetramer interface, two β-strands associate to form a wide antiparallel β-sheet of eight β-strands. Due to the presence of the nonconserved Pro^{29} that bends the first β-strand, the two adjacent β-strands are hydrogen-bonded only via water molecules. The molecular surface area of the β-interchanged suc1 dimer inaccessible to a water-sized, 1.4-Å-radius probe sphere in this tetramer conformation is 650 $Å^2$, a value slightly lower than that promoted by zinc (862 $Å^2$; ref. 18), suggesting that this is a weak interaction. The tetramerization interface between the two β-interchanged suc1 dimers resembles the zinc-promoted interface observed between monomers in the β-hairpin single-domain suc1 structure (18) except that there is a translation of 15 Å along the N-terminal β-strand direction (Figs. 1*C* and 2*A*).

The existence of two crystallographically independent β-interchanged dimers within the asymmetric unit allows comparison both to other suc1-homolog structures and between the two independent β-interchanged suc1 dimers (Fig. 2*A*). When the two distinct suc1 folds are compared, the hinge points are localized within the residue triad Val^{89}-Pro^{90}-Glu^{91} by rotational movements in (ϕ,ψ) dihedral angles (Fig. 2*B*). In contrast, superposition of one suc1 monomer with the equivalent in the CksHs2 dimer structure reveals a different locus of the β-hinge region, located in the residue pairs Pro^{62}-Glu^{63} and Pro^{64}-His^{65} in CksHs2 (Pro^{90}-Glu^{91} and Pro^{92}-His^{93} in suc1) (Fig. 2*B*). Therefore, the adjacent subunit in CksHs2 is located in approximately the same orientation, but in opposite directions as compared with the β-interchanged suc1 dimer. Superposition of the two β-interchanged suc1 dimers within the crystallographic asymmetric unit gives the striking result that each HVPEPH region has a somewhat different conformation (Fig. 2*C*). Considered alone, the structures of the core are virtually superimposable, with a rmsd of 0.55 Å for main-chain atoms, but the hinge bending angle between the cores differs by 25° in a direction roughly perpendicular to the C^α–C^α vector of the residue pair Val^{89}-Pro^{90}, verifying that this is, in fact, a flexible hinge.

The suc1 β-hinge region is well ordered and reveals low temperature factors in the β-interchanged suc1 dimer crystal structure, indicating that these suc1 residues are not especially mobile or disordered (Fig. 2*D*). In contrast, high temperature factors (>40 $Å^2$ compared with an average of 28 $Å^2$) indicate high flexibility for CksHs2 in the region Glu^{61}–His^{65} (Val^{89}–His^{93} in suc1). Pairs of conserved Glu^{63} (Glu^{91} in suc1) side chains adjacent in the middle of the interchanged β-strands (19) destabilize the CksHs2 dimer and hexamer at neutral and higher pH. In the β-strand-swapped suc1 dimer, a hydrophobic cluster resulting from the close packing of Val^{87} and Val^{89} from each subunit forms a stable interface. Thus, the association of the CksHs2 dimer into a hexamer may be needed to compensate for its electrostatically destabilized β-hinge conformation. However, the β-interchanged suc1 can be purified as a dimer, and no molecular assemblies larger than dimer or weak tetramer were observed by gel filtration experiments for suc1 from fission yeast. These results suggest that a β-interchanged suc1 dimer represents a stable conformation, that trimerization into the hexamer observed in CksHs2 (19) is not necessary

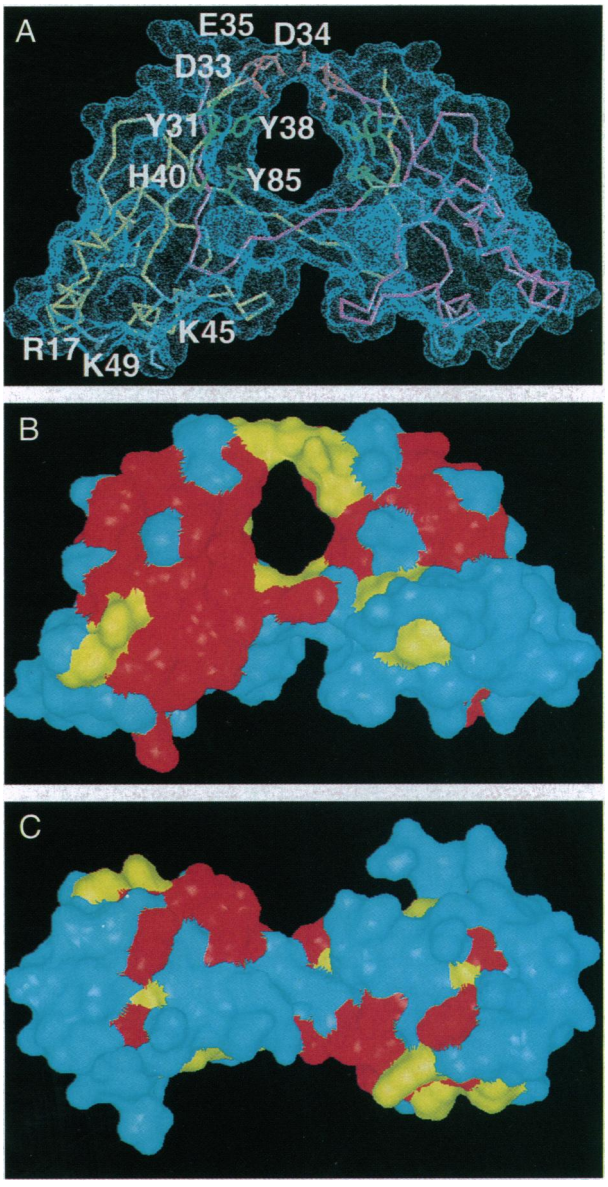

FIG. 3. Molecular surface of the β-interchanged suc1 dimer showing the conserved aromatic and acidic residues within the dimer channel. (*A*) Molecular surface for the β-interchanged suc1 dimer (blue points) with the C^α trace (yellow and magenta) and the conserved clusters of green (Tyr^{31}, Tyr^{38}, His^{40}, and Tyr^{85}) aromatic side chains and of pink (Asp^{33}, Asp^{34}, and Glu^{35}) negatively charged side chains. Two clusters of positively charged residues (blue Arg^{17}, Lys^{45}, and Lys^{49} side chains) are positioned along one face of the dimer. The tyrosine cluster and the negatively charged and positively charged residues are labeled for one subunit (left). (*B*) Sequence conservation and variation at the molecular surface (red, invariant; yellow, highly conserved; and blue, nonconserved residues) is viewed looking down into the central solvent-filled channel. The sequence-invariant residues defined in *A* within and around this channel lie on each face of the β-interchanged suc1 dimer. (*C*) The view rotated 90° from that in *B*, showing that there are no other large conserved patches of residues at the molecular surface of the β-interchanged suc1 dimer.

for β-interchanged dimer formation, and that suc1 conformational change involves a true molecular hinge and not a completely flexible loop.

Besides the β-hinge-controlled conformational change, the suc1 dimer structure reveals an anion binding site with implications for molecular recognition. In each subunit of the β-interchanged suc1 dimer, a conserved patch of positively charged residues (Arg^{30}, Arg^{39}, and Arg^{99}) along with Trp^{82} and Ser^{79} form an anion binding site, which is inaccessible to solvent because of the adjacent subunit packing in the tetramer. As a result, a chloride ion is sequestered into the anion binding site and is tightly bound to the side chains of Trp^{82} and Arg^{99} and to the Ser^{79} N atom from one subunit, as well as to the Thr^{77} side chain from an adjacent subunit in the crystal (Fig. 2*E*).

The significance of the β-hinge-mediated dimer for Cdk binding is apparent from alteration of the conserved accessible surface (Fig. 3). A patch of sequence-conserved tyrosine residues (Tyr^{31}, Tyr^{38}, and Tyr^{85}) is sequestered in the β-interchanged suc1 dimer at the periphery of a small solvent-filled channel (Fig. 3). The close proximity of six negatively charged residues (Asp^{33}, Asp^{34}, and Glu^{35} from each subunit) closes this ring structure (Fig. 3*A*). In both suc1 and CksHs2, the narrow channel diameter (10–12 Å) limits binding of proteins such as Cdk. In contrast, these same residues are fully accessible to Cdk or other proteins in the closed β-hairpin conformation of the suc1 β-hinge. For molecular interactions, the β-interchanged suc1 dimer conformation also positions two sets of three positively charged residues (Arg^{17}, Lys^{45}, and Lys^{49}), which are located in protruding α-helices of each subunit, on the same side of the β-interchanged suc1 dimer (Fig. 3*A*) for possible protein recognition.

DISCUSSION

The existence of two distinct conformation and assembly states for the same suc1 protein sequence is relevant to studies of both protein folding and suc1 biological activity. The β-interchanged suc1 dimer and the trimer of CksHs2 each create a solvent-filled channel surrounded by the homologous patch of residues (Tyr^{31}, Tyr^{38}, Tyr^{85}, and His^{40}) which, together with the conserved Asp^{33} (Asp^{14} in CksHs2), may contribute to a binding site for a calcium ion or other metal ion (19). The cluster of conserved positively charged residues on suc1 (Arg^{30}, Arg^{39}, and Arg^{99}) that bind chloride ion may represent an anion recognition site.

The suc1 β-interchanged dimer and β-hairpin single-domain folds of suc1 provide significant differences in conserved accessible molecular surface and, thus, a structural basis for altering suc1 functional interactions. Such large conformational changes in proteins are known to occur in response to the binding of ligands (see, for example, refs. 28–30) and the cleavage of serpins (31) and in proteins such as immunoglobulins (32). Identical hexapeptide sequences have also been observed in different conformations in proteins (33). However, to our knowledge, a flexible hinge that can open into an extended form and close into a β-bend, allowing interconversions of domain conformation and dimer assembly of a same protein, is a novel motif and structural mechanism. Yet the molecular mechanism of suc1 conversion between β-strand closing and opening conformations does resemble the mechanism of domain swapping noted in a few oligomeric enzymes (ref. 21 and references therein). Thus, the β-strand domain swapping observed here is analogous to the interchange of the N-terminal segment observed in the dimeric bovine seminal RNase (20).

The structural differences defined here between the β-hairpin single-domain and β-interchanged dimer structures indicate that these suc1 regulatory proteins could adapt their conformation and assembly in response to environmental changes occurring at precise times during the cell cycle. These results thus suggest a structural mechanism for regulation of Cdk kinase function based upon cooperative changes in suc1 conformation and assembly. Biochemical, genetic, and structural characterizations of suc1–Cdk assembly states will be needed to establish the basis for regulation of Cdk function by suc1 and to reconcile the various genetically inferred roles for suc1 proteins in cell cycle progression. The structural results presented here provide the basis for site-directed mutagenesis aimed at probing the role of the β-hinge motif, the aromatic cluster, the anion binding site, and β-strand domain swapping in suc1 biological function.

We thank N.-H. Xuong for access to the University of California, San Diego, Research Resource for Protein Crystallography and P. Russell, C. D. Stout, and E. D. Getzoff for discussions.

1. Pines, J. & Hunter, T. (1991) *Trends Cell Biol.* **1,** 117–121.
2. Hunter, T. (1993) *Cell* **75,** 839–841.
3. Dunphy, W. G. (1994) *Trends Cell Biol.* **4,** 202–207.
4. Hadwiger, J. A., Wittenberg, C., Mendenhall, M. D. & Reed, S. I. (1989) *Mol. Cell. Biol.* **9,** 2034–2041.
5. Lohka, M. J., Hayes, M. K. & Maller, J. L. (1988) *Proc. Natl. Acad. Sci. USA* **85,** 3009–3013.
6. Brizuela, L., Draetta, G. & Beach, D. (1989) *Proc. Natl. Acad. Sci. USA* **86,** 4362–4366.
7. Meikrantz, W., Suprynowicz, F. A., Halleck, M. S. & Schlegel, R. A. (1990) *Proc. Natl. Acad. Sci. USA* **87,** 9600–9604.
8. Kusubata, M., Tokui, T., Matsuoka, Y., Okumura, E., Tachibana, K., Hisanaga, S., Kishimoto, T., Yasuda, H., Kamijo, M., Ohba, Y., Tsujimura, K., Yatani, R. & Inagaki, M. (1992) *J. Biol. Chem.* **267,** 20937–20942.
9. Colas, P., Serras, F. & van Loon, A. E. (1993) *Int. J. Dev. Biol.* **37,** 589–594.
10. Richardson, H. E., Stueland, C. S., Thomas, J., Russell, P. & Reed, S. I. (1990) *Genes Dev.* **4,** 1332–1334.
11. Tang, Y. & Reed, S. I. (1993) *Genes Dev.* **7,** 822–832.
12. Hayles, J., Aves, S. & Nurse, P. (1986) *EMBO J.* **5,** 3373–3379.
13. Hayles, J., Beach, D., Durkacz, B. & Nurse, P. (1986) *Mol. Gen. Genet.* **202,** 291–293.
14. Hindley, J., Phear, G., Stein, M. & Beach, D. (1987) *Mol. Cell. Biol.* **7,** 504–511.
15. Moreno, S., Hayles, J. & Nurse, P. (1989) *Cell* **58,** 361–372.
16. Dunphy, W. G. & Newport, J. W. (1988) *Cell* **55,** 925–928.
17. Dunphy, W. G. & Newport, J. W. (1989) *Cell* **58,** 181–191.
18. Endicott, J. A., Noble, M. E., Garman, E. F., Brown, N., Rasmussen, B., Nurse, P. & Johnson, L. N. (1995) *EMBO J.* **14,** 1004–1014.
19. Parge, H. E., Arvai, A. S., Murtari, D. J., Reed, S. I. & Tainer, J. A. (1993) *Science* **262,** 387–395.
20. Piccoli, R., Tamburrini, M., Piccialli, G., Di Donato, A., Parente, A. & D'Alessio, G. (1992) *Proc. Natl. Acad. Sci. USA* **89,** 1870–1874.
21. Bennett, M. J., Choe, S. & Eisenberg, D. (1994) *Proc. Natl. Acad. Sci. USA* **91,** 3127–3131.
22. Matthews, B. W. (1968) *J. Mol. Biol.* **33,** 491–497.
23. Hamlin, R. (1985) *Methods Enzymol.* **114,** 416–452.
24. Navaza, J. (1994) *Acta Crystallogr. Sect. A Fundam. Crystallogr.* **50,** 157–163.
25. Brünger, A. T., Kuriyan, J. & Karplus, M. (1987) *Science* **235,** 458–460.
26. Roussel, A. & Cambillau, C. (1989) in *Silicon Graphics Geometry Partners Directory* (Silicon Graphics, Mountain View, CA), pp. 77–78.
27. Carson, M. (1991) *J. Appl. Crystallogr.* **24,** 958–961.
28. Johnson, L. N., Acharya, K. R., Jordan, M. D. & McLaughlin, P. J. (1990) *J. Mol. Biol.* **211,** 645–661.
29. Faber, H. R. & Matthews, B. W. (1990) *Nature (London)* **348,** 263–265.
30. Anderson, B. F., Baker, H. M., Norris, G. E., Rumball, S. V. & Baker, E. N. (1990) *Nature (London)* **344,** 784–787.
31. Banzon, J. A. & Kelly, J. W. (1992) *Protein Eng.* **5,** 113–115.
32. Harris, L. J., Larson, S. B., Hasel, K. W., Day, J., Greenwood, A. & McPherson, A. (1992) *Nature (London)* **360,** 369–372.
33. Cohen, B. I., Presnell, S. R. & Cohen, F. E. (1993) *Protein Sci.* **2,** 2134–2145.